

Hidden Scale Invariance in Polydisperse Mixtures of Exponential Repulsive Particles

Trond S. Ingebrigtsen,* Thomas B. Schröder, and Jeppe C. Dyre*

Cite This: *J. Phys. Chem. B* 2021, 125, 317–327

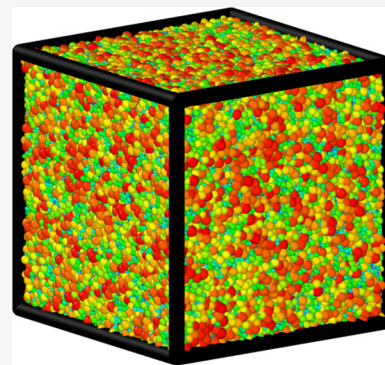
Read Online

ACCESS |

Metrics & More

Article Recommendations

ABSTRACT: Polydisperse systems of particles interacting by the purely repulsive exponential (EXP) pair potential are studied in regard to how structure and dynamics vary along isotherms, isochores, and isomorphs. The sizable size polydispersities of 23%, 29%, 35%, and 40%, as well as energy polydispersity 35%, were considered. For each system an isomorph was traced out covering about one decade in density. For all systems studied, the structure and dynamics vary significantly along the isotherms and isochores but are invariant to a good approximation along the isomorphs. We conclude that the single-component EXP system's hidden scale invariance (implying isomorph invariance of structure and dynamics) is maintained even when a sizable polydispersity is introduced into the system.



INTRODUCTION

The EXP pair potential is defined by the purely repulsive exponential function

$$v_{\text{EXP}}(r) = \epsilon e^{-r/\sigma} \quad (1)$$

Although systems of particles interacting with this pair potential have been studied much less than, for example, the Lennard-Jones^{1–3} or inverse-power-law pair-potential systems,⁴ papers reporting investigations of the EXP system or, more generally, systems that involve a repulsive EXP term in the pair potential have appeared regularly over a period of many years.^{5–18} The EXP system deserves an in-depth study for two reasons. First, real-world systems like the low-density limit of the Yukawa (screened Coulomb) system is well described by the EXP pair potential, which is also an ingredient in many empirical potentials used for describing metals. Second, the EXP pair potential is the “mother of all pair potentials” in a recent explanation of the quasiuniversality that characterizes the structure and dynamics of simple liquids.^{19,20} Any pair potential, even an oscillatory one, that can be written as a sum of EXP terms with coefficients much larger than $k_{\text{B}}T$ defines a system in the quasiuniversality class defined by the hard-sphere, inverse-power-law, and Lennard-Jones (LJ) type systems.^{19,20} For this class the following applies: different systems at thermodynamic state points with the same excess entropy have virtually the same reduced-unit structure and dynamics.^{19–21} Consequently, if one prefers analytic pair potentials, the EXP pair-potential system is suited to replace the hard-sphere system as the generic system in liquid-state theory.²⁰

Providing a thorough study of the single-component EXP system motivated four recent papers.^{22–25} The first paper²² studied the EXP system's isotherms and isochores in the fluid phase. This encompasses both a typical gas-like region and a typical liquid-like region (because the EXP system is purely repulsive, no phase transition separates these two regions; there is merely a gradual transition). An example of quasiuniversality was also given in ref 22, demonstrating almost identical reduced pair distribution function for the LJ and the EXP systems at state points with the same reduced diffusion coefficient. The second paper²³ presented simulation data for three isomorphs (configurational adiabats) and showed that structure and dynamics in reduced units are invariant along isomorphs, each of which covered one decade of density variation, i.e., much larger than what is realistic in experiments. This means that the EXP system obeys the “hidden scale invariance” symmetry that effectively makes the thermodynamic phase diagram one-dimensional instead of two-dimensional in regard to structure and dynamics.^{26–28} A third paper in the series²⁴ presented the thermodynamic phase diagram of the EXP system and identified its melting line, showing that it is an approximate isomorph.^{26,29} That paper also demonstrated that the solid phase has two stable

Received: October 27, 2020

Revised: December 6, 2020

Published: December 28, 2020



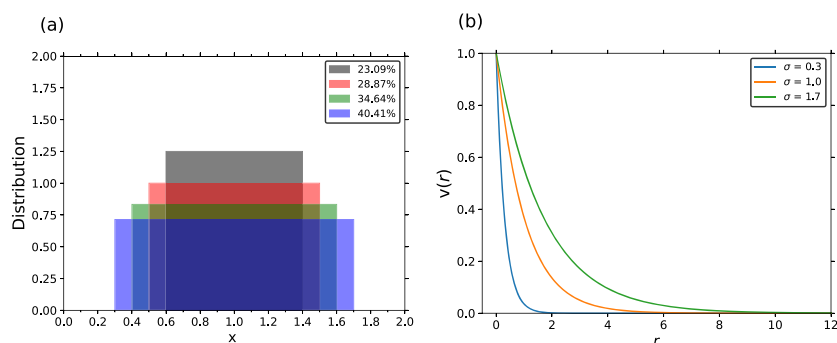


Figure 1. (a) Box distributions used in the simulations of polydisperse EXP systems where x is either σ or ε relative to its average. (b) Range of the EXP potentials for $\delta = 40\%$ size polydispersity (the figure uses MD units; see eq 8). Note the significant polydispersity with the σ of the EXP pair potentials varying by almost a factor of 6.

crystalline structures, a face-centered cubic structure at low densities and a body-centered cubic structure at higher densities. The fourth single-component EXP paper²⁵ studied isomorphs in the solid phase, demonstrating isomorph invariance of structure and dynamics in both crystalline phases.

While previous investigations of the EXP pair potential all involved single-component systems, many experimental samples are multicomponent systems, e.g., colloids³⁰ and dirty plasmas.³¹ Polydispersity has been discussed in connection with the dynamics of glass-forming liquids³² and the issue of defining configurational entropy,³³ and theories have been proposed for an effective one-component description of the structure of a polydisperse system.³⁰ Indeed, from a purely theoretical point of view such systems present interesting physics on their own; e.g., novel features in their phase behavior³⁴ and, for instance, melting has been studied of a face-centered crystalline solid consisting of polydisperse LJ spheres with Gaussian size polydispersity.³⁵

Polydisperse systems of particles interacting by purely repulsive inverse power-law (IPL) pair potentials $\propto r^{-12}$ have highly nontrivial properties. Thus, in 2010 Sollich and Wilding showed that systems of dense polydisperse IPL spheres may phase separate into coexisting face-centered cubic phases, tracking up to four coexisting phases depending on the degree of polydispersity.³⁶ Each of these phases is “fractionated” in the sense that it involves a narrower distribution of particle sizes than that of the overall system. This is, in fact, a common characteristic of polydisperse systems.

More recently, polydispersity has been discussed for hard-sphere systems^{37,38} and come into focus because of the significant speedup obtained by applying the swap algorithm for these systems.³⁹ It is therefore of interest to investigate whether the single-component EXP system’s hidden scale invariance, the prerequisite for having isomorphs,^{20,23,26,28} survives for polydisperse systems of EXP particles. Work by one of us on the LJ system, which also has hidden scale invariance and thus isomorphs, showed that the LJ system’s hidden scale invariance survives the introduction of continuous polydispersity.^{40,41} In this paper we present data from simulations of polydisperse mixtures of particles interacting via the EXP pair potential subject to the Lorentz–Berthelot mixing rules,⁴² demonstrating that the same applies for the EXP pair-potential system. Since the EXP system as mentioned may be regarded as the prototype liquid pair potential that explains simple liquids’ quasiuniversality,²⁰ this finding

suggests a possible path to understanding the quasiuniversality of mixtures, a subject of current interest.⁴³

Hidden scale invariance is the property that the ordering of configurations according to their potential energy is maintained under a uniform compression or extension. If \mathbf{R} is the vector of all particle coordinates and $U(\mathbf{R})$ is the potential-energy function, the mathematical definition of hidden scale invariance is²⁸

$$U(\mathbf{R}_a) < U(\mathbf{R}_b) \Rightarrow U(\lambda\mathbf{R}_a) < U(\lambda\mathbf{R}_b) \quad (2)$$

Here λ is a parameter quantifying the uniform scaling. It is understood that the configurations \mathbf{R}_a and \mathbf{R}_b are of the same density. Although no realistic system obeys eq 2 rigorously, for many systems in the liquid and solid phases including the Yukawa, LJ-type, and EXP systems, eq 2 applies to a good approximation for most configurations when λ is not far from unity. This implies that isomorphs exist in the thermodynamic phase diagram, which are defined as lines of constant excess entropy and characterized by the property that structure and dynamics in reduced units are invariant along an isomorph to a good approximation.²⁸

A system that obeys hidden scale invariance (eq 2) to a good approximation for most of its configurations is termed Roskilde (R)-simple. Such systems are simple because their thermodynamic phase diagram is effectively one-dimensional in regard to structure and dynamics. It is believed that most metals and van der Waals bonded systems are R-simple in their liquid and solid phases, whereas most systems with strong directional bonds like covalent or hydrogen-bonded systems are not. Note that the class of R-simple systems on the one hand includes molecular systems but on the other hand excludes some pair-potential systems; thus this class differs from the standard “simple liquids” defined as pair-potential systems. It should be mentioned that, among several other regularities, isomorph theory explains Rosenfeld’s excess-entropy scaling from 1977.^{21,44} For more on the isomorph theory and its validation in computer simulations and experiments, the reader is referred to the reviews given in refs 20, 21, 27, and 45.

The EXP system is R-simple in the entire low-temperature part of its phase diagram.^{19,22} This implies good invariance of structure and dynamics along the isomorphs. One may think of the single-component EXP system as being well approximated by an IPL system with an exponent that is not constant, but increases as density is decreased.²² If the EXP potential is to be generalized to describing mixtures and systems with non-isotropic interactions, several EXP parameters σ and ε will

need to be involved. That a mapping to an effective IPL system is possible for polydisperse EXP systems is not obvious, in particular at high polydispersity, because of the dependence of the effective IPL exponent on particle distance and thus on the EXP interaction parameters.

To investigate whether polydisperse EXP systems maintain the hidden-scale-invariance property of the single-component EXP system, we present below extensive simulation data for five polydisperse mixtures of EXP particles. The conclusion is that isomorphs do exist for such mixtures, even at high polydispersity. This applies for both size and energy polydispersity. The main focus of the paper is on size polydispersity because this is the most common form of polydispersity realized, e.g., in colloidal suspensions and micelles, as well as on the molecular level in polymers, bitumen, etc. It should be noted, however, that polydisperse systems are gaining increasing attention as models, e.g., for biological systems.^{41,46}

THEORETICAL METHODS

This section provides definitions and details of the computer simulations.

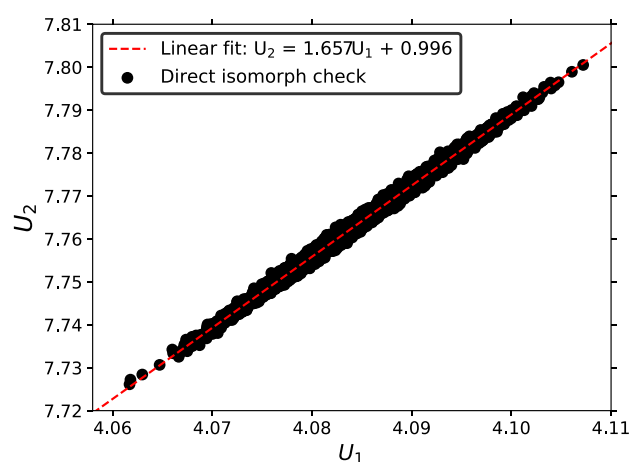


Figure 2. Example of the direct-isomorph-check method for tracing out an isomorph. This case involves 40% polydispersity and considers a jump from $(\rho_1, T_1) = (10^{-3}, 10^{-4})$ to the higher density $\rho_2 = 1.25 \times 10^{-3}$ for which the temperature T_2 is sought such that (ρ_1, T_1) and (ρ_2, T_2) are on the same isomorph. The dashed line gives the best fit slope from which T_2/T_1 is obtained (note that the best fit line is not supposed to pass through the origin because one may well have $C_{12} \neq 1$ in eq 9).

Polydispersity. Size polydispersity involves a mixture of particles, each of which is associated with the same energy

parameter ε (eq 1) and a potential-length parameter σ selected from a probability distribution. In this work we use for simplicity the uniform “box” probability distribution. One could also have used a Gaussian parameter distribution, but there is little reason to expect qualitative differences between different distributions. The relevant property is how far the system is from being monodisperse.

Following the standard convention, the polydispersity measure δ is defined⁴⁷ as the ratio between standard deviation and average, i.e.,

$$\delta \equiv \frac{\sqrt{\langle(\Delta\sigma)^2\rangle}}{\langle\sigma\rangle} \quad (3)$$

in which $\Delta\sigma \equiv \sigma - \langle\sigma\rangle$ and sharp brackets denote averages. For the uniform distribution, $\sigma_a < \sigma < \sigma_b$, one finds $\langle\sigma\rangle = (\sigma_a + \sigma_b)/2$ and $\langle\sigma^2\rangle = (\sigma_b^3 - \sigma_a^3)/3(\sigma_b - \sigma_a) = (\sigma_a^2 + \sigma_a\sigma_b + \sigma_b^2)/3$. Since $\langle(\Delta\sigma)^2\rangle = \langle\sigma^2\rangle - \langle\sigma\rangle^2$, the polydispersity is given by $\delta^2 = \langle\sigma^2\rangle/\langle\sigma\rangle^2 - 1 = (4/3)(\sigma_a^2 + \sigma_a\sigma_b + \sigma_b^2)/(\sigma_b + \sigma_a)^2 - 1 = (1/3)(\sigma_b - \sigma_a)^2/(\sigma_b + \sigma_a)^2$, i.e.,

$$\delta = \frac{1}{\sqrt{3}} \frac{\sigma_b - \sigma_a}{\sigma_b + \sigma_a} \quad (4)$$

It follows that the maximum polydispersity of the uniform distribution is $1/\sqrt{3}$, which is 57.7%.

Figure 1a shows the distributions of our study, while Figure 1b illustrates how different the involved EXP pair potentials are for the highest size polydispersity studied (40%). This polydispersity roughly sets the limit for when it is possible to equilibrate the system.

The energy polydispersity parameter δ is defined by an expression analogous to eq 3,

$$\delta \equiv \frac{\sqrt{\langle(\Delta\varepsilon)^2\rangle}}{\langle\varepsilon\rangle} \quad (5)$$

which for the uniform distribution $\varepsilon_a < \varepsilon < \varepsilon_b$ leads to

$$\delta = \frac{1}{\sqrt{3}} \frac{\varepsilon_b - \varepsilon_a}{\varepsilon_b + \varepsilon_a} \quad (6)$$

For both types of polydispersity, the standard Lorentz–Berthelot mixing rules were employed,⁴² i.e., the interaction between particle i and particle j is described by an EXP pair potential with $\sigma = (\sigma_i + \sigma_j)/2$ and $\varepsilon = \sqrt{\varepsilon_i\varepsilon_j}$.

Unit Systems. Two unit systems are used below. Isomorph theory uses the so-called reduced units.²⁶ If N particles in a volume V are considered in thermal equilibrium at the temperature T , the (number) density is defined by $\rho \equiv N/V$ and the length, energy, and time units are,²⁶ respectively,

Table 1. Characteristics of the Five Isomorphs Studied, Four with Size Polydispersity and One with Energy Polydispersity^a

polydispersity δ (%)	parameter range	max/min ratio	reference state point	figure number
23.09	$0.6 < \sigma < 1.4$	2.3	$\rho = 2 \times 10^{-4}, T = 1 \times 10^{-6}$	5
28.87	$0.5 < \sigma < 1.5$	3.0	$\rho = 1 \times 10^{-5}, T = 1 \times 10^{-4}$	6
34.64	$0.4 < \sigma < 1.6$	4.0	$\rho = 1 \times 10^{-3}, T = 1 \times 10^{-4}$	7
40.41	$0.3 < \sigma < 1.7$	5.7	$\rho = 1 \times 10^{-3}, T = 1 \times 10^{-4}$	8
34.64	$0.4 < \varepsilon < 1.6$	4.0	$\rho = 1 \times 10^{-3}, T = 1 \times 10^{-4}$	9

^aIn all cases a uniform parameter distribution was invoked. The size and energy polydispersity parameter δ is defined in eq 3 and eq 5, respectively. Isomorphs were generated by the direct-isomorph-check method based on eq 9, starting from the reference state point and moving both up and down in density.

$$\rho^{-1/3}, \quad k_B T, \quad \rho^{-1/3} \sqrt{\frac{m}{k_B T}} \quad (7)$$

Structure and dynamics are reported in reduced units because the isomorph theory predicts invariance of structure and dynamics only in these (state-point dependent) units, not in fixed “real” or MD (molecular dynamics) units.^{21,26,28}

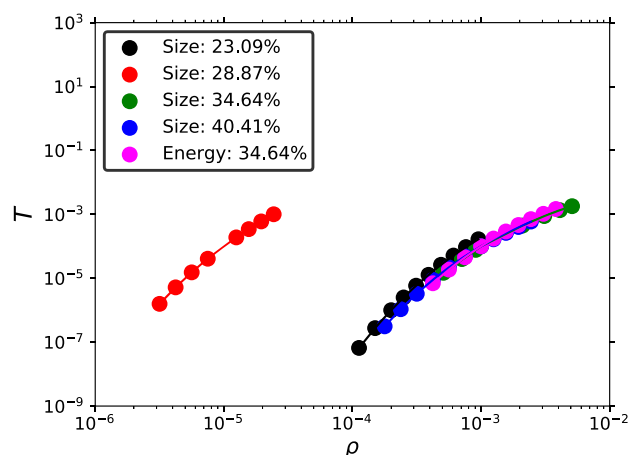


Figure 3. Simulated isomorphs plotted in the log-scale density–temperature phase diagram (MD units, eq 8). Even though four out of five isomorphs are close to each other in this diagram, the physics varies significantly from isomorph to isomorph due to the widely varying polydispersities involved, compare Figures 6–9.

MD units are used below for specifying the temperature and density at the thermodynamic state point in question because in reduced units ρ and T are both equal to 1. The MD length, energy, and time units used are, respectively,

$$\langle \sigma \rangle, \quad \langle \varepsilon \rangle, \quad \langle \sigma \rangle \sqrt{\frac{m}{\langle \varepsilon \rangle}} \quad (8)$$

Here $\langle \sigma \rangle$ and $\langle \varepsilon \rangle$ are the averages of σ and ε . This unit system applies in all cases studied; for instance in the case of size polydispersity ε is constant and accordingly $\langle \varepsilon \rangle = \varepsilon$. The MD temperature unit is $\langle \varepsilon \rangle / k_B$.

Below, quantities reported in reduced units are marked by a tilde, e.g., the pair distance r is in reduced unit given as $\tilde{r} \equiv \rho^{1/3} r$. Quantities without a tilde are given in MD units.

Simulation Details. The simulations employed standard Nose-Hoover NVT molecular dynamics with periodic boundary conditions.⁴² Simulations were performed by GPU (graphics cards) computing using the open-source Roskilde University Molecular Dynamics (RUMD) package.⁴⁸ All particle masses m were identical, with $m = 1$ in MD units. A shifted-force cutoff⁴⁹ at the reduced pair distance $\tilde{r} = 8$ was used for all simulations, implying that the cutoff in MD units is equal to $8\rho^{-1/3}$, which is a density-dependent cutoff. The reduced-unit time step was 0.0025 in all simulations. Each state point was simulated for at least 25 million time steps for equilibration and a similar number of time steps for production runs. All simulations involved $N = 32\,000$ particles. This relatively large number ensures that results are reproducible in the sense that a different sample with the same parameter distribution results in basically the same results, which is why the reported results are for a single sample. Finite-size effects

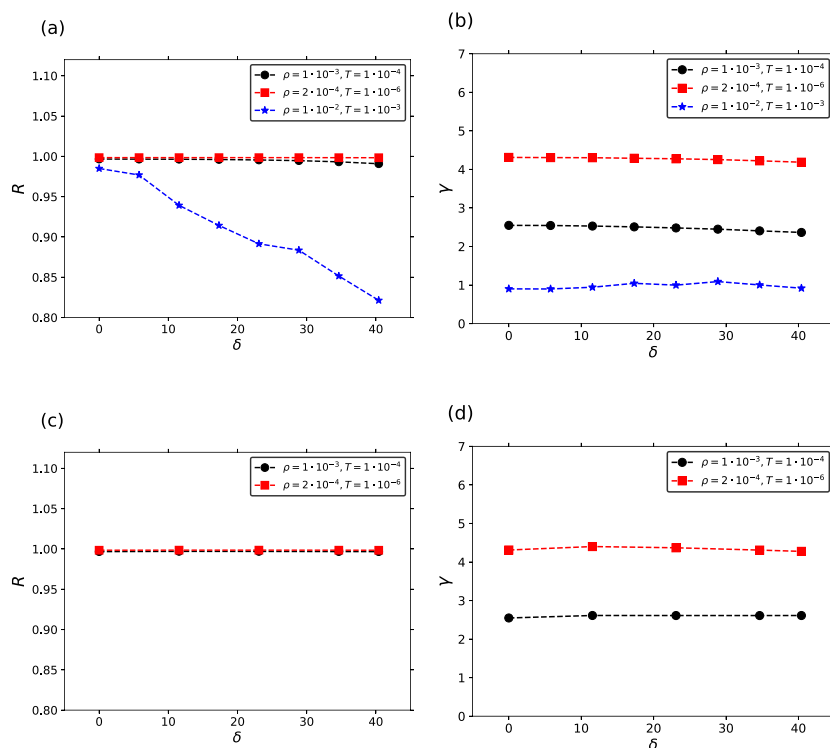


Figure 4. Virial potential-energy correlation coefficient R (eq 10) and density-scaling exponent γ (eq 11) plotted as a function of polydispersity at selected state points. (a) and (b) show R and γ for size-polydisperse systems, while (c) and (d) show R and γ for energy-polydisperse systems. $\delta = 0$ corresponds to the single-component EXP system, which has strong correlations in the entire low-temperature part of its phase diagram.²²

Size polydispersity 23.09%

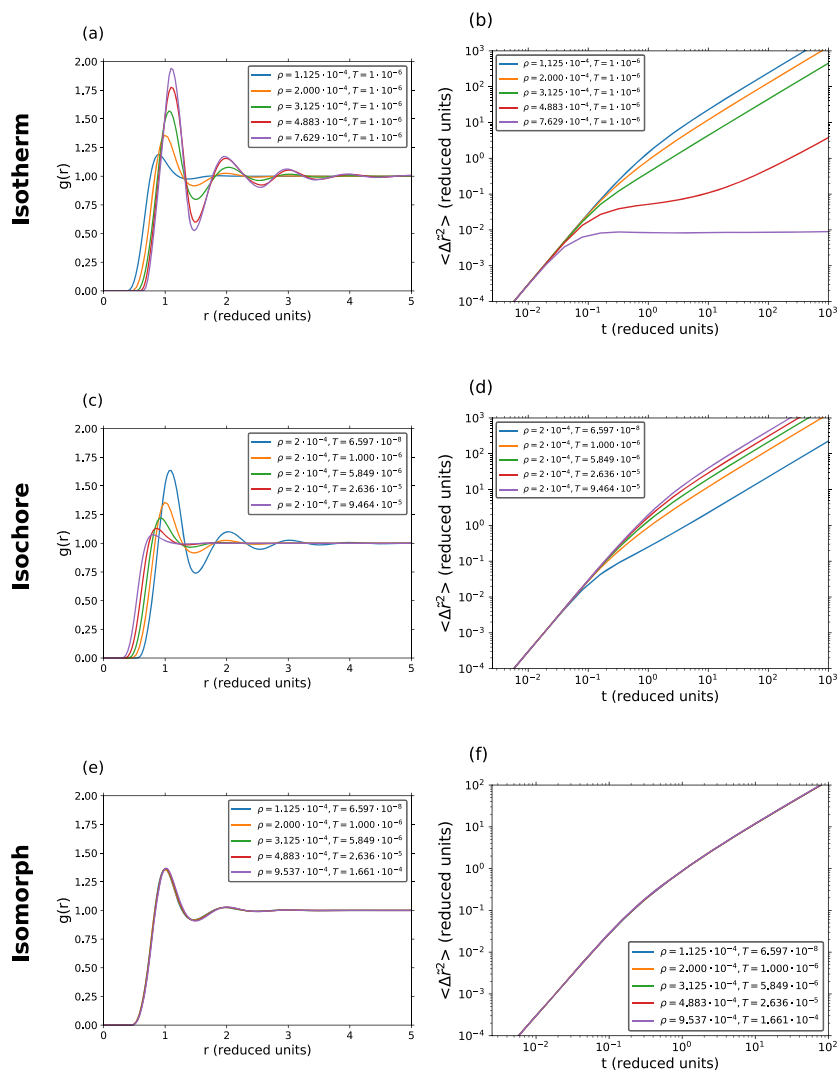


Figure 5. Size polydispersity $\delta = 23.09\%$ corresponding to the max/min size ratio 2.3 (Table 1). The reference state point is $(\rho, T) = (2 \times 10^{-4}, 1 \times 10^{-6})$. The radial and time coordinates are given in reduced units (eq 7). (a) and (b) give radial distribution function (RDF) and mean-square displacement (MSD) data for the $T = 1 \times 10^{-6}$ isotherm. (c) and (d) give analogous data for the $\rho = 2 \times 10^{-4}$ isochore. (e) and (f) give data for the reference-state-point isomorph, demonstrating a good invariance of both structure and dynamics.

coming from variations in the distributed parameters were observed only at very high polydispersity, and here only for systems significantly smaller than those studied.

How Isomorphs Are Traced Out Numerically. An isomorph is defined as a curve of constant excess entropy in the thermodynamic phase diagram of an R-simple system.²⁸ Different methods may be used for identifying isomorphs in a computer simulation.^{26,50,51} We used the so-called direct-isomorph-check,²⁶ which is based on the following reasoning. Consider two configurations \mathbf{R}_1 and \mathbf{R}_2 of density ρ_1 and ρ_2 , respectively, which can be scaled uniformly into one another ($\rho_1^{1/3}\mathbf{R}_1 = \rho_2^{1/3}\mathbf{R}_2$). It can be shown from eq 2²⁸ that if \mathbf{R}_1 and \mathbf{R}_2 are typical equilibrium configurations of the state points (ρ_1, T_1) and (ρ_2, T_2) , then these two configurations have proportional canonical Boltzmann probabilities (below, C_{12} is a constant determined by the state points, i.e., independent of the configurations):

$$e^{-U(\mathbf{R}_1)/(k_B T_1)} = C_{12} e^{-U(\mathbf{R}_2)/(k_B T_2)} \quad (\rho_1^{1/3}\mathbf{R}_1 = \rho_2^{1/3}\mathbf{R}_2) \quad (9)$$

It can be shown that two state points (ρ_1, T_1) and (ρ_2, T_2) obeying eq 9 have the same excess entropy,²⁶ i.e., belong to the same isomorph. Given the state point (ρ_1, T_1) and the density ρ_2 , eq 9 provides a method for determining T_2 , working as follows: From an equilibrium simulation at (ρ_1, T_1) several configurations are selected. Each of these is scaled uniformly to density ρ_2 . By plotting the potential energy of scaled versus unscaled configurations, a scatter plot with strong correlations is obtained, the slope of which according to eq 9 is T_2/T_1 .²⁶ An example is given in Figure 2.

The isomorphs studied below were generated by the direct-isomorph-check method involving 25% density changes, starting from a selected “reference” state point and moving both up and down in density. The reference state points are listed in Table 1, which also gives the polydispersity

Size polydispersity 28.87%

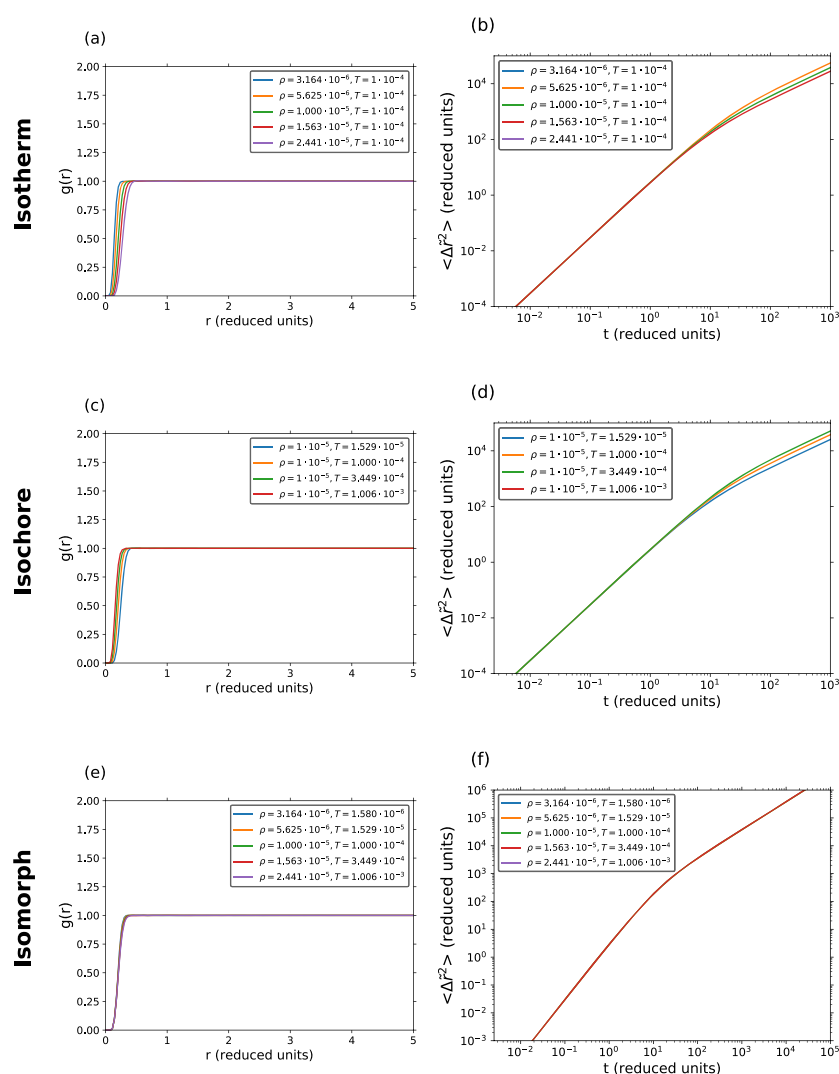


Figure 6. Size polydispersity $\delta = 28.87\%$ corresponding to the max/min size ratio 3.0. The reference state point is $(\rho, T) = (1 \times 10^{-5}, 1 \times 10^{-4})$, which is a gas-like state point. (a) and (b) show data for the $T = 1 \times 10^{-4}$ isotherm covering a density range of a factor of ~ 8 . (c) and (d) show data for the $\rho = 1 \times 10^{-5}$ isochore covering a temperature range of a factor of ~ 70 . There is a visible variation of both structure and dynamics, although not as significant as in Figure 5. (e) and (f) demonstrate approximate isomorph invariance of structure and dynamics for the reference-state-point isomorph covering a density variation of ~ 8 and a temperature variation of ~ 600 .

characteristics. Each isomorph covers a density variation of almost a full decade.

Before the generation of isomorphs can be undertaken, it is important to ensure that the system does not phase-separate or crystallize. This was done by visual inspection of selected configurations, as well as by monitoring the average potential energy that drops significantly whenever a system simulated by *NVT* dynamics crystallizes.

RESULTS AND DISCUSSION

Virial Potential-Energy Correlations and the Density-Scaling Exponent. As mentioned already, the single-component EXP system obeys hidden scale invariance (eq 2) in the entire low-temperature part of its phase diagram, meaning that the system is here R-simple in the gas–liquid (fluid) as well as solid phases. Isomorph theory applies only when there is hidden scale invariance to a good approximation.

A measure of when this is the case is the virial potential-energy Pearson correlation coefficient R defined⁵² by

$$R \equiv \frac{\langle \Delta U \Delta W \rangle}{\sqrt{\langle (\Delta U)^2 \rangle \langle (\Delta W)^2 \rangle}} \quad (10)$$

Here U is the potential energy, W is the virial (excess-pressure) function defined by $W(\mathbf{R}) = \sum_{i < j} \mathbf{r}_{ij} \cdot \mathbf{F}_{ij} / 3$ in which \mathbf{r}_{ij} is the position vector from particle i to particle j and \mathbf{F}_{ij} is the force with which particle i acts on particle j .^{2,42} Δ denotes the quantity in question minus its state-point average, and the sharp brackets denote *NVT* (canonical) averages. By convention, a system is R-simple (“strongly correlating”) whenever $R > 0.9$.⁵² Although this is a somewhat arbitrary criterion, it provides a useful rule of thumb for determining whether or not a given system has good isomorphs in the investigated region of the phase diagram.

Size polydispersity 34.64%

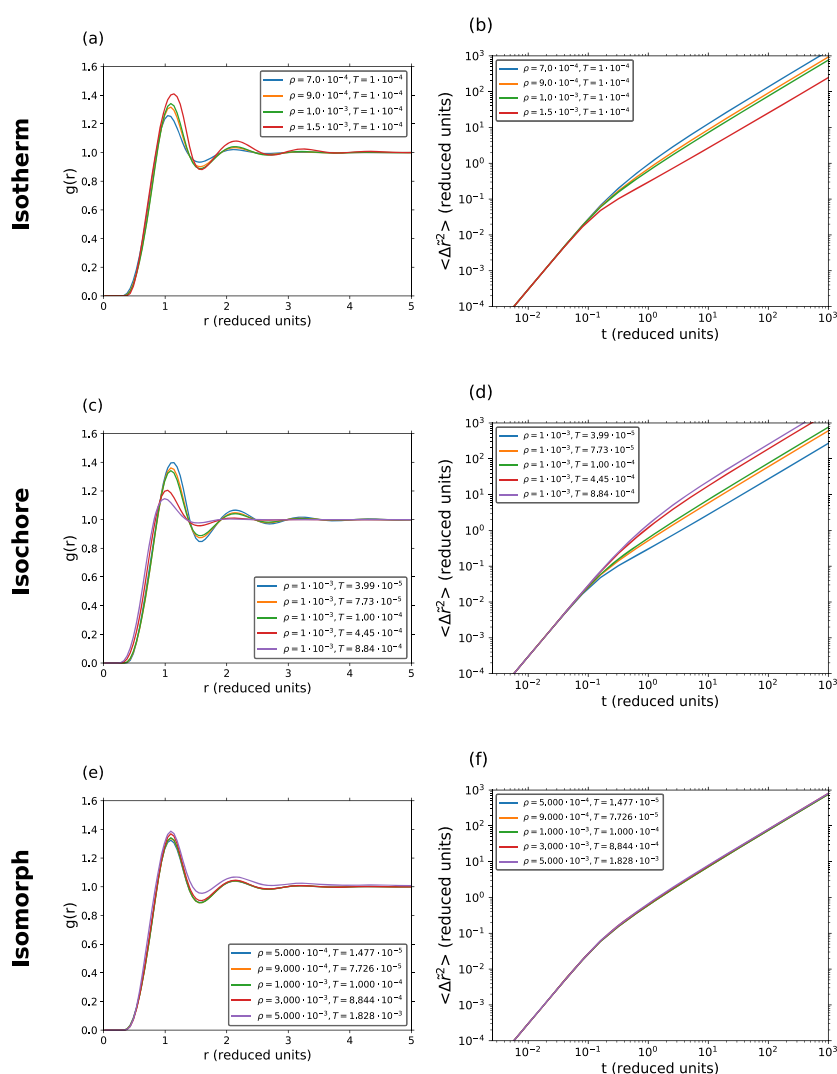


Figure 7. Data for size polydispersity $\delta = 34.64\%$ corresponding to the max/min size ratio 4.0. The reference state point is $(\rho, T) = (1 \times 10^{-3}, 1 \times 10^{-4})$. (a) and (b) show data for the $T = 1 \times 10^{-4}$ isotherm covering a density range of a factor of ~ 2 . (c) and (d) show data for the $\rho = 1 \times 10^{-3}$ isochore covering a temperature range of a factor of ~ 20 . (e) and (f) demonstrate approximate isomorph invariance of structure and dynamics for the reference-state-point isomorph covering a density variation of a decade and a temperature variation of ~ 120 .

If a system is R-simple and thus has isomorphs, an important characteristic is the so-called density-scaling exponent γ that gives the isomorph slope in the logarithmic density–temperature phase diagram (see Figure 3 and eq 11).^{26,27,53} By definition, isomorphs have constant excess entropy and γ is defined²⁶ by (in which the second equality is the generally valid statistical-mechanical identity used to calculate γ from constant-density canonical-ensemble equilibrium fluctuations²⁶)

$$\gamma \equiv \left(\frac{\partial \ln T}{\partial \ln \rho} \right)_{S_{\text{ex}}} = \frac{\langle \Delta U \Delta W \rangle}{\langle (\Delta U)^2 \rangle} \quad (11)$$

In general, γ is state-point-dependent.^{50,51,54,55} If γ were a constant, however, the isomorphs would be characterized by a constant ρ^γ/T ,^{53,56} which is the origin of the name “density-scaling exponent”. A high density-scaling exponent signals harshly repulsive forces; indeed $\gamma = n/3$ for the system of

particles interacting via pair potentials $\propto r^{-n}$ in which n is the inverse power-law exponent.⁴

Figure 4 shows how R and γ vary as a function of the size ((a) and (b)) and energy ((c) and (d)) polydispersity parameter δ . Data are shown for three size and two energy polydisperse state points. Except for the relatively high-density and high-temperature state point data (blue stars), R and γ vary little from their pure EXP-system ($\delta = 0$) values and the systems are R-simple. The blue stars show that size-polydisperse systems stop being R-simple at large polydispersity if the temperature is (relatively) high. At such high densities and temperatures we found, in fact, that samples often crystallized partially during the simulation for which reason we excluded that part of the phase diagram from the study.

Isotherms, Isochores, and Isomorphs in Four Size-Polydisperse Systems. This section presents data for systems with size polydispersity 23%, 29%, 35%, and 40%. The structure is probed by the radial distribution function

Size polydispersity 40.41%

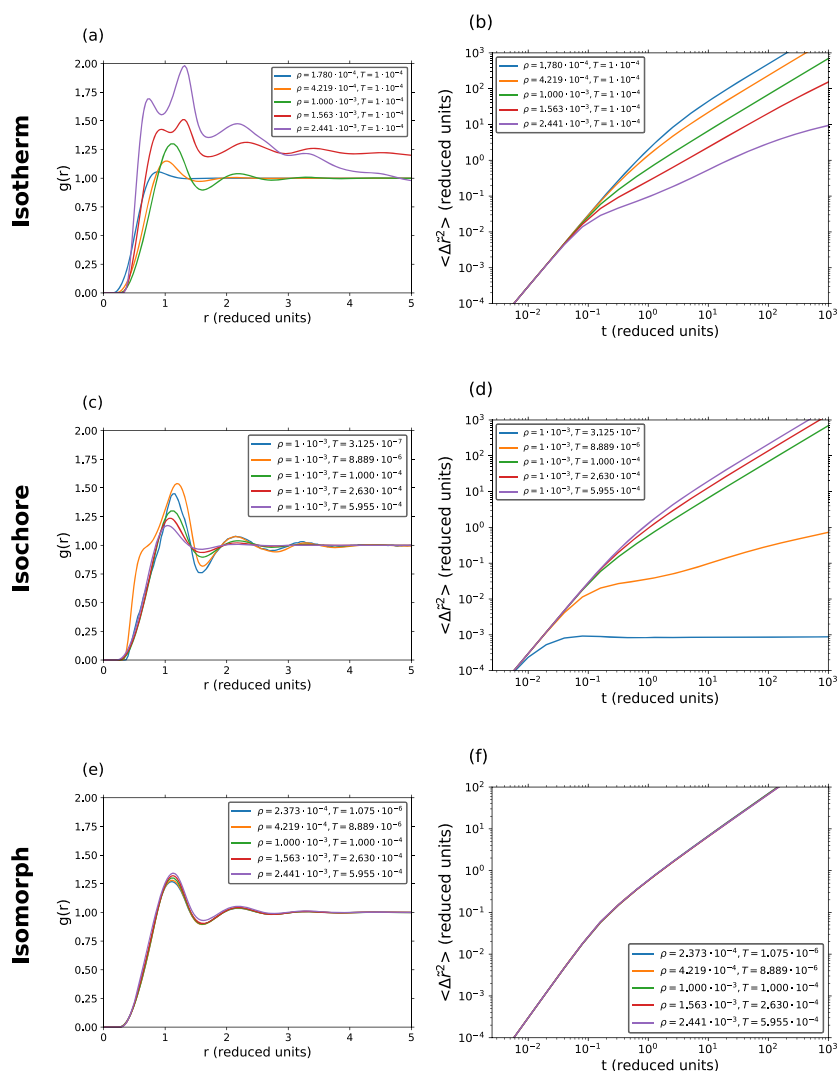


Figure 8. Data for size polydispersity $\delta = 40.41\%$ corresponding to the max/min size ratio 5.7. The reference state point is $(\rho, T) = (1 \times 10^{-3}, 1 \times 10^{-4})$. As discussed in the text, a few state points of the isotherms and isochores show qualitative deviations, reflecting phase separation and/or crystallization. Except for this, the picture is much like that of the previous figures. (a) and (b) show data for the $T = 1 \times 10^{-4}$ isotherm covering a density range of a factor of ~ 14 . (c) and (d) show data for the $\rho = 1 \times 10^{-3}$ isochore covering a temperature range of a factor of ~ 200 . (e) and (f) demonstrate approximate isomorph invariance of structure and dynamics for the reference-state-point isomorph covering a density variation of ~ 10 and a temperature variation of ~ 600 .

(RDF), which is denoted by $g(r)$ and plotted as a function of the reduced radial distance $\tilde{r} \equiv \rho^{1/3}r$. The dynamics is probed by the mean-square displacement as a function of time, $\langle \Delta r^2(t) \rangle$, which is also plotted in reduced units.

For each polydispersity we selected a reference state point in relation to which six subfigures are presented. The two top figures give reference-state-point isotherm data at different densities for the RDF and the MSD, respectively. The middle two figures give reference-state-point isochore (i.e., constant-volume) data at different temperatures for the RDF and the MSD. The two lower figures give data for the reference-state-point isomorph. Each isomorph covers roughly one decade of density variation. This is much larger than in realistic experiments, as mentioned, but it allows for a critical test of the predicted isomorph invariance. Figure 3 shows a phase diagram with the isomorphs studied.

Figure 5 shows data for the smallest size polydispersity, 23%, which nevertheless corresponds to more than a factor of 10 “volume” variation between the particles (the max/min σ ratio is 2.3, compare Table 1, which is similar to the variation among the metallic elements). Figure 5a and Figure 5b show data for the $T = 1 \times 10^{-6}$ isotherm covering a density range of ~ 7 (the symbol \sim is here used in the meaning “roughly equal to”). Figure 5c and Figure 5d show data for the $\rho = 2 \times 10^{-4}$ isochore covering a temperature range of ~ 1400 . In all four cases there is a considerable variation of both structure and dynamics. The two final figures, Figure 5e and Figure 5f, demonstrate good isomorph invariance of structure and dynamics in the same part of the phase diagram for similar density and temperature variations. There is a good though not perfect collapse of the data, reflecting the fact that the isomorph theory is not exact except in the physically unrealistic

Energy polydispersity 34.64%

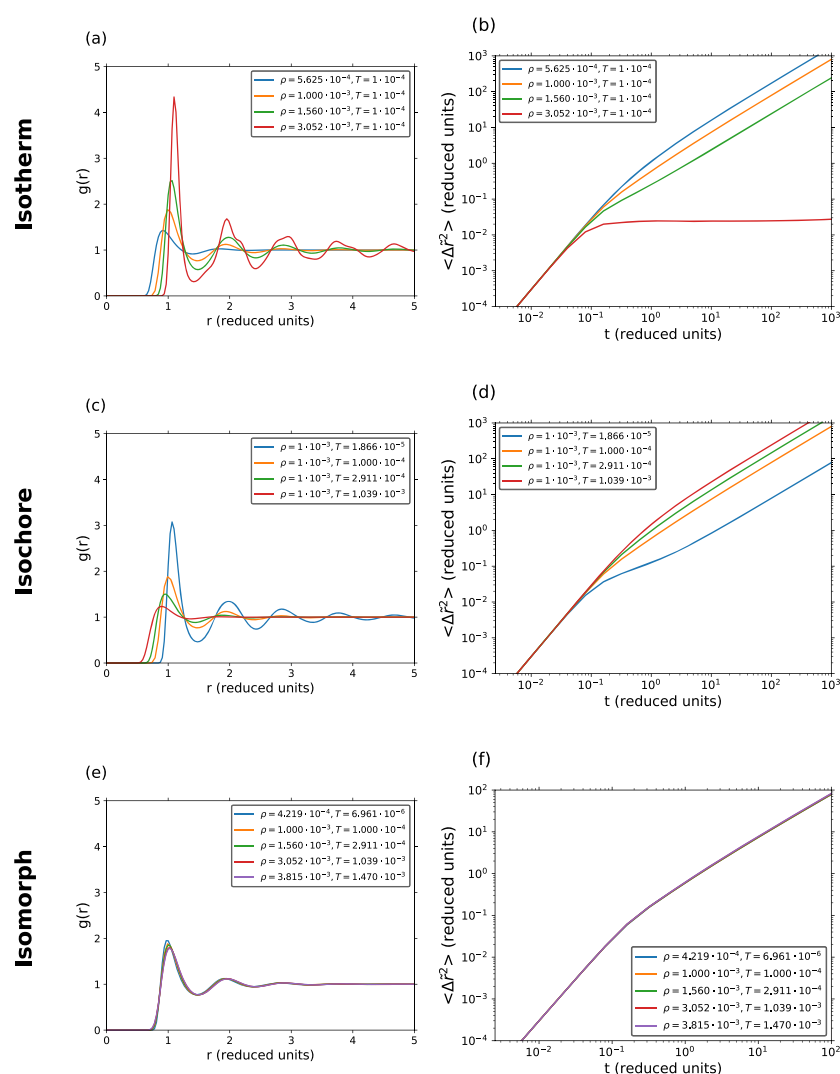


Figure 9. Energy polydispersity $\delta = 34.64\%$ corresponding to max/min energy ratio of 4.0. The reference state point is $(\rho, T) = (1 \times 10^{-3}, 1 \times 10^{-4})$. (a) and (b) show data for the $T = 1 \times 10^{-4}$ isotherm covering a density range of a factor ~ 5 . (c) and (d) show data for the $\rho = 1 \times 10^{-3}$ isochore covering a temperature range of a factor of ~ 50 . (e) and (f) demonstrate approximate isomorph invariance of structure and dynamics for the reference-state-point approximate isomorph covering a density variation of ~ 10 and a temperature variation of ~ 200 .

case of an Euler-homogeneous potential-energy function,²⁸ a case that includes all inverse power-law pair potentials.

Figure 6 shows analogous data for size polydispersity 29%, corresponding to almost a factor of 30 volume variation from the smallest to the largest EXP particles. Compared to Figure 5, these data are taken at much lower densities and much higher temperatures, i.e., at much more gas-like states, as evidenced by the lack of structure in the RDF. While most R-simple liquids, e.g., the LJ liquid, have a virial potential-energy correlation coefficient R much below 0.9 in the gas phase and consequently have no isomorphs here, the single-component EXP system is an interesting exception, which has excellent isomorphs in the entire low-temperature region, also for gas-like state points.^{22,23} Figure 6 demonstrates that this applies also for size-polydisperse EXP systems.

Figure 7 shows data for size polydispersity 35% corresponding to more than a factor of 60 volume variation of the particles. Again we find significant changes of structure and dynamics along the isotherms and isochores but good

invariance along the isomorph. The highest density and temperature state points on the isomorph (purple curve) deviate in its structure from the others; this state point has the poorest virial potential-energy correlation, compare Figure 4a. A systematic deviation from isomorph invariance is seen for the height of the first RDF peak (Figure 7e). This is also observed, although to a lesser extent, for the other isomorphs of this paper, as well as for single-component systems including the EXP system.²³ We have generally found that the first RDF maximum always increases slightly when moving along an isomorph in the direction of increasing γ . In our interpretation, this is because the single-pair Boltzmann probability factor at short distance is proportional to $\exp[-v(r)/(k_B T)]$ which is not isomorph invariant, and this Boltzmann factor is smaller the steeper the potential is, i.e., the larger γ is. As a consequence, if the total area under the first RDF peak is isomorph invariant reflecting an isomorph-invariant coordination number, in order to compensate for the short-distance

“loss”, the RDF peak value can be expected to increase with increasing γ .

The final size-polydispersity figure is for $\delta = 40\%$ (Figure 8), corresponding to a factor of ~ 200 volume variation among the particles. The data follow the same picture as for smaller polydispersities, although we now find signs of a phase separation at the highest density isothermal state points (Figure 8a) and of crystallization at the lowest temperature isochoric state point (indicated by the constant MSD in Figure 8d). Overall, the RDF is still isomorph invariant, although to a lesser extent than for systems with smaller polydispersity. The polydispersity under study here, however, goes much beyond normal experimental conditions. The fact that invariance is observed even at such extreme polydispersity illustrates the robustness of isomorph theory.

Results for an Energy-Polydisperse System. As mentioned in the Introduction, varying the particle size is most relevant for modeling realistic experimental mixtures. For completeness, however, we have also simulated an EXP energy-polydisperse system. Reference 41 showed that isomorph theory applies for energy polydisperse LJ mixtures. Figure 9 shows EXP energy polydispersity data plotted in the same way as for the size polydisperse systems. Also in this case the simulations demonstrate approximate isomorph invariance of structure and dynamics. The data show changes along both the isotherms and the isochores, which are larger than for the size-polydisperse system with the same δ (Figure 7). This reflects the significantly larger density and temperature variations.

CONCLUSIONS

This paper has demonstrated that polydisperse systems of EXP particles are R-simple and have good isomorph invariance of both structure and dynamics. This means that the single-component EXP system's hidden scale invariance demonstrated in ref 23 applies also if size or energy variations are introduced, even if these are quite significant. This finding is not trivial because the effective inverse-power-law exponent describing the EXP pair potential depends on the distance relative to σ (increasing as the pair distance increases), which implies that size-polydisperse mixtures involve a range of effective inverse power-law interactions. Previous results by one of us dealing with the LJ system demonstrated that introducing either size⁴⁰ or energy⁴¹ polydispersity did not ruin the hidden scale invariance of the standard LJ system. In view of the above demonstration that the same applies for the EXP system, we conclude that the hidden-scale-invariance property is robust to polydispersity. As mentioned, this is far from trivial, and it would be desirable to have a better analytical understanding of this fact. Thus, while methods exist for estimating the density-scaling exponent γ from the pair potential of R-simple single-component pair-potential systems,^{51,57} for polydisperse systems there is no theory or even approximate analytical method for estimating the virial potential-energy correlation coefficient R and the density-scaling exponent γ . The fact that γ does not change much with polydispersity (Figure 4) indicates that the same theory might be applied; validating this presents an important challenge for future work.

AUTHOR INFORMATION

Corresponding Authors

Trond S. Ingebrigtsen – Glass and Time, IMFUFA, Department of Science and Environment, Roskilde University, DK-4000 Roskilde, Denmark; Email: trond@ruc.dk

Jeppe C. Dyre – Glass and Time, IMFUFA, Department of Science and Environment, Roskilde University, DK-4000 Roskilde, Denmark; orcid.org/0000-0002-0770-5690; Email: dyre@ruc.dk

Author

Thomas B. Schröder – Glass and Time, IMFUFA, Department of Science and Environment, Roskilde University, DK-4000 Roskilde, Denmark

Complete contact information is available at:

<https://pubs.acs.org/10.1021/acs.jpcb.0c09726>

Notes

The authors declare no competing financial interest.

ACKNOWLEDGMENTS

This work was supported by the VILLUM Foundation's Matter Grant 16515.

REFERENCES

- (1) Lennard-Jones, J. E. On the determination of molecular fields. I. From the variation of the viscosity of a gas with temperature. *Proc. R. Soc. London A* **1924**, *106*, 441–462.
- (2) Hansen, J.-P.; McDonald, I. R. *Theory of Simple Liquids: With Applications to Soft Matter*, 4th ed.; Academic: New York, 2013.
- (3) Heyes, D. M.; Dini, D.; Branka, A. C. Scaling of Lennard-Jones liquid elastic moduli, viscoelasticity and other properties along fluid-solid coexistence. *Phys. Status Solidi B* **2015**, *252*, 1514–1525.
- (4) Heyes, D. M.; Branka, A. C. Self-diffusion coefficients and shear viscosity of inverse power fluids: from hard- to soft-spheres. *Phys. Chem. Chem. Phys.* **2008**, *10*, 4036–4044.
- (5) Morse, P. M. Diatomic molecules according to the wave mechanics. II. Vibrational levels. *Phys. Rev.* **1929**, *34*, 57–64.
- (6) Born, M.; Mayer, J. E. Zur Gittertheorie der Ionenkristalle. *Eur. Phys. J. A* **1932**, *75*, 1–18.
- (7) Buckingham, R. A. The classical equation of state of gaseous helium, neon and argon. *Proc. R. Soc. London A* **1938**, *168*, 264–283.
- (8) Buckingham, R. A.; Corner, J. Tables of second virial and low-pressure Joule-Thompson coefficients for intermolecular potentials with exponential repulsion. *Proc. R. Soc. A* **1947**, *189*, 118–129.
- (9) Mason, E. A.; Vanderslice, J. T. Calculation of virial and Joule-Thomson coefficients at extremely high temperatures. *Ind. Eng. Chem.* **1958**, *50*, 1033–1035.
- (10) Girifalco, L. A.; Weizer, V. G. Application of the Morse potential function to cubic metals. *Phys. Rev.* **1959**, *114*, 687–690.
- (11) Monchick, L. Collision integrals for the exponential repulsive potential. *Phys. Fluids* **1959**, *2*, 695–700.
- (12) Kac, M.; Uhlenbeck, G. E.; Hemmer, P. C. On the van der Waals theory of the vapor-liquid equilibrium. I. Discussion of a one-dimensional model. *J. Math. Phys.* **1963**, *4*, 216–228.
- (13) Sherwood, A. E.; Mason, E. A. Virial coefficients for the exponential repulsive potential. *Phys. Fluids* **1965**, *8*, 1577–1579.
- (14) Henderson, D.; Oden, L. Asymptotic formulas for the virial coefficients using the exponential repulsive potential. *Phys. Fluids* **1966**, *9*, 1592–1594.
- (15) Tang, K. T.; Toennies, J. P. An improved simple model for the van der Waals potential based on universal damping functions for the dispersion coefficients. *J. Chem. Phys.* **1984**, *80*, 3726–3741.
- (16) Jacobsen, K. W.; Stoltze, P.; Nørskov, J. K. A semi-empirical effective medium theory for metals and alloys. *Surf. Sci.* **1996**, *366*, 394–402.

- (17) Chakraborty, S. N.; Chakravarty, C. Entropy, local order, and the freezing transition in Morse liquids. *Phys. Rev. E* **2007**, *76*, 011201.
- (18) Maimbourg, T.; Kurchan, J. Approximate scale invariance in particle systems: A large-dimensional justification. *EPL* **2016**, *114*, 60002.
- (19) Bacher, A. K.; Schröder, T. B.; Dyre, J. C. Explaining why simple liquids are quasi-universal. *Nat. Commun.* **2014**, *5*, 5424.
- (20) Dyre, J. C. Simple liquids' quasiuniversality and the hard-sphere paradigm. *J. Phys.: Condens. Matter* **2016**, *28*, 323001.
- (21) Dyre, J. C. Perspective: Excess-entropy scaling. *J. Chem. Phys.* **2018**, *149*, 210901.
- (22) Bacher, A. K.; Schröder, T. B.; Dyre, J. C. The EXP pair-potential system. I. Fluid phase isotherms, isochores, and quasiuniversality. *J. Chem. Phys.* **2018**, *149*, 114501.
- (23) Bacher, A. K.; Schröder, T. B.; Dyre, J. C. The EXP pair-potential system. II. Fluid phase isomorphs. *J. Chem. Phys.* **2018**, *149*, 114502.
- (24) Pedersen, U. R.; Bacher, A. K.; Schröder, T. B.; Dyre, J. C. The EXP pair-potential system. III. Thermodynamic phase diagram. *J. Chem. Phys.* **2019**, *150*, 174501.
- (25) Bacher, A. K.; Pedersen, U. R.; Schröder, T. B.; Dyre, J. C. The EXP pair-potential system. IV. Isotherms, isochores, and isomorphs in the two crystalline phases. *J. Chem. Phys.* **2020**, *152*, 094505.
- (26) Gnan, N.; Schröder, T. B.; Pedersen, U. R.; Bailey, N. P.; Dyre, J. C. Pressure-energy correlations in liquids. IV. "Isomorphs" in liquid phase diagrams. *J. Chem. Phys.* **2009**, *131*, 234504.
- (27) Dyre, J. C. Hidden scale invariance in condensed matter. *J. Phys. Chem. B* **2014**, *118*, 10007–10024.
- (28) Schröder, T. B.; Dyre, J. C. Simplicity of condensed matter at its core: Generic definition of a Roskilde-simple system. *J. Chem. Phys.* **2014**, *141*, 204502.
- (29) Pedersen, U. R.; Costigliola, L.; Bailey, N. P.; Schröder, T. B.; Dyre, J. C. Thermodynamics of freezing and melting. *Nat. Commun.* **2016**, *7*, 12386.
- (30) Pond, M. J.; Errington, J. R.; Truskett, T. M. Implications of the effective one-component analysis of pair correlations in colloidal fluids with polydispersity. *J. Chem. Phys.* **2011**, *135*, 124513.
- (31) Chaudhuri, M.; Ivlev, A. V.; Khrapak, S. A.; Thomas, H. M.; Morfill, G. E. Complex plasma – the plasma state of soft matter. *Soft Matter* **2011**, *7*, 1287–1298.
- (32) Abraham, S. E.; Bhattacharyya, S. M.; Bagchi, B. Energy landscape, antiplasticization, and polydispersity induced crossover of heterogeneity in supercooled polydisperse liquids. *Phys. Rev. Lett.* **2008**, *100*, 167801.
- (33) Ozawa, M.; Parisi, G.; Berthier, L. Configurational entropy of polydisperse supercooled liquids. *J. Chem. Phys.* **2018**, *149*, 154501.
- (34) Sollich, P. Predicting phase equilibria in polydisperse systems. *J. Phys.: Condens. Matter* **2002**, *14*, R79–R117.
- (35) Sarkar, S.; Biswas, R.; Santra, M.; Bagchi, B. Solid-liquid transition in polydisperse Lennard-Jones systems. *Phys. Rev. E* **2013**, *88*, 022104.
- (36) Sollich, P.; Wilding, N. B. Crystalline Phases of Polydisperse Spheres. *Phys. Rev. Lett.* **2010**, *104*, 118302.
- (37) Ogarko, V.; Luding, S. Prediction of polydisperse hard-sphere mixture behavior using tridisperse systems. *Soft Matter* **2013**, *9*, 9530–9534.
- (38) Santos, A.; Yuste, S. B.; de Haro, M. L.; Ogarko, V. Equation of state of polydisperse hard-disk mixtures in the high-density regime. *Phys. Rev. E: Stat. Phys., Plasmas, Fluids, Relat. Interdiscip. Top.* **2017**, *96*, 062603.
- (39) Ninarello, A.; Berthier, L.; Coslovich, D. Models and algorithms for the next generation of glass transition studies. *Phys. Rev. X* **2017**, *7*, 021039.
- (40) Ingebrigtsen, T. S.; Tanaka, H. Effect of size polydispersity on the nature of Lennard-Jones liquids. *J. Phys. Chem. B* **2015**, *119*, 11052–11062.
- (41) Ingebrigtsen, T. S.; Tanaka, H. Effect of energy polydispersity on the nature of Lennard-Jones liquids. *J. Phys. Chem. B* **2016**, *120*, 7704–7713.
- (42) Allen, M. P.; Tildesley, D. J. *Computer Simulation of Liquids*; Oxford Science Publications: Oxford, U.K., 1987.
- (43) Bell, I. H.; Dyre, J. C.; Ingebrigtsen, T. S. Excess-entropy scaling in supercooled binary mixtures. *Nat. Commun.* **2020**, *11*, 4300.
- (44) Rosenfeld, Y. Relation between the transport coefficients and the internal entropy of simple systems. *Phys. Rev. A: At., Mol., Opt. Phys.* **1977**, *15*, 2545–2549.
- (45) Ingebrigtsen, T. S.; Schröder, T. B.; Dyre, J. C. What is a simple liquid? *Phys. Rev. X* **2012**, *2*, 011011.
- (46) Shagolsem, L. S.; Rabin, Y. Particle dynamics in fluids with random interactions. *J. Chem. Phys.* **2016**, *144*, 194504.
- (47) Frenkel, D.; Vos, R. J.; de Kruif, C. G.; Vrij, A. Structure factors of polydisperse systems of hard spheres: A comparison of Monte Carlo simulations and Percus–Yevick theory. *J. Chem. Phys.* **1986**, *84*, 4625–4630.
- (48) Bailey, N. P.; Ingebrigtsen, T. S.; Hansen, J. S.; Veldhorst, A. A.; Böhling, L.; Lemarchand, C. A.; Olsen, A. E.; Bacher, A. K.; Costigliola, L.; Pedersen, U. R.; et al. RUMD: A general purpose molecular dynamics package optimized to utilize GPU hardware down to a few thousand particles. *Scipost Phys.* **2017**, *3*, 038.
- (49) Toxvaerd, S.; Dyre, J. C. Communication: Shifted forces in molecular dynamics. *J. Chem. Phys.* **2011**, *134*, 081102.
- (50) Böhling, L.; Ingebrigtsen, T. S.; Grzybowski, A.; Paluch, M.; Dyre, J. C.; Schröder, T. B. Scaling of viscous dynamics in simple liquids: Theory, simulation and experiment. *New J. Phys.* **2012**, *14*, 113035.
- (51) Böhling, L.; Bailey, N. P.; Schröder, T. B.; Dyre, J. C. Estimating the density-scaling exponent of a monatomic liquid from its pair potential. *J. Chem. Phys.* **2014**, *140*, 124510.
- (52) Bailey, N. P.; Pedersen, U. R.; Gnan, N.; Schröder, T. B.; Dyre, J. C. Pressure-energy correlations in liquids. I. Results from computer simulations. *J. Chem. Phys.* **2008**, *129*, 184507.
- (53) Roland, C. M.; Hensel-Bielowka, S.; Paluch, M.; Casalini, R. Supercooled dynamics of glass-forming liquids and polymers under hydrostatic pressure. *Rep. Prog. Phys.* **2005**, *68*, 1405–1478.
- (54) Fragiadakis, D.; Roland, C. M. Intermolecular distance and density scaling of dynamics in molecular liquids. *J. Chem. Phys.* **2019**, *150*, 204501.
- (55) Sanz, A.; Hecksher, T.; Hansen, H. W.; Dyre, J. C.; Niss, K.; Pedersen, U. R. Experimental evidence for a state-point-dependent density-scaling exponent of liquid dynamics. *Phys. Rev. Lett.* **2019**, *122*, 055501.
- (56) Alba-Simionesco, C.; Cailliaux, A.; Alegria, A.; Tarjus, G. Scaling out the density dependence of the alpha relaxation in glass-forming polymers. *Europhys. Lett.* **2004**, *68*, 58–64.
- (57) Bailey, N. P.; Pedersen, U. R.; Gnan, N.; Schröder, T. B.; Dyre, J. C. Pressure-energy correlations in liquids. II. Analysis and consequences. *J. Chem. Phys.* **2008**, *129*, 184508.